Journal of the Korean Ceramic Society
Vol. 29, No. 12, PP. 949~955, 1992.

# R-Curve Behavior in a Gas-Pressure Sintered Silicon Nitride

**Sang S. Kim, Sung J. Kim and Sunggi Baik**
Department of Materials Science and Engineering
Pohang Institute of Science and Technology (POSTECH)
(Received October 31, 1992)

# 가스압 소결된 질화규소의 R-Curve 거동

김상섭 · 김성진 · 백성기
포항공과대학 재료 · 금속공학과
(1992년 10월 31일 접수)

## ABSTRACT

R-curves, fracture resistance ($K_R$) as a function of crack extension ($\Delta a$), of a gas-pressure sintered monolithic $Si_3N_4$ were determined by controlled flaw/strength technique. Rising R-curve behavior was observed, confirming the operation of microstructural toughening process during crack growth. The R-curve parameters, k and m in the equation, $K_R=k(\Delta a)^m$, were determined to 30.301 and 0.1146, respectively. Microstructural observation of growing crack revealed that the bridging in the crack wake by unbroken ligament of large elongated β-grains was the mechanism primarily for the rising R-curve behavior.

## 요 약

가스압 소결된 질화규소의 R-curve, 즉 균열전파($\Delta a$)에 따른 파괴인성($K_R$)의 변화 거동을 controlled flaw/strength법으로 조사하였다. 균열의 길이가 증가함에 따라 파괴인성도 증가하는 양상이 관찰되었고, 이는 균열이 진행하는 동안 균열의 성장을 억제하는 강화기구가 작용한다는 것을 나타낸다. R-curve를 기술하는 식, $K_R=k(\Delta a)^m$에서 k와 m은 각각 30.301과 0.1146으로 계산되었다. 균열진행부의 미세구조를 관찰한 결과 균열후단에서의 미균열된 큰 주상형의 β상에 의한 bridging 효과가 R-curve 현상을 유발한 주요 강화기구로 판단되었다.

## 1. Introduction

It has been shown[1-4] that some ceramic materials exhibit increasing crack growth resistance with crack extension. R-curve behavior of stabilized zirconia[1,2] has been attributed to phase transformation in the advancing crack front. Bridging and frictional pull-out of whisker/fiber reinforcement in the crack wake are found to be responsible for strong R-curve behavior in silicon carbide whisker reinforced alumina[3]. Recently, bridging grains in the crack wake was found to be contributing the R-curves in coarse-grained alumina[4]. Ceramics with steeply rising R-curve characteristics have high potential for greater reliability due to smaller strength variability, i.e., a higher Weibull modulus.

Typical monolithic polycrystalline silicon nitride materials have shown fracture toughness in the range of 4~6 $MPa\cdot m^{1/2}$ [5]. High toughnesses have been attributed to the whisker-like morphology of β-silicon nitride grains which deflect the crack front effectively[6]. Tani *et al.*[7] recently showed that the fracture toughness of monolithic $Si_3N_4$ can be as high as 9 $MPa\cdot m^{1/2}$ when its microstructure contains some large β-$Si_3N_4$ grains with high aspect ratios. Their experimental silicon nitride material showed extensive evidence of crack deflection.

Such monolithic $Si_3N_4$ can be considered as an in-situ grown whisker-reinforced material, which might be expected to show various toughening processes like crack deflection, whisker pullout, or crack bridging. As

a result, it has been expected to show strong R-curve behavior in one form or another.

R-curve behaviors have been indeed demonstrated in various monolithic $Si_3N_4$ ceramics. Li and Yamanis[8] characterized the R-curves in a gas-pressure-sintered $Si_3N_4$ using double cantilever beam (DCB) method and indentation/fracture strength (IFS) measurements method. They found that the R-curve parameters, k and m in the equation, $K_R=k(\Delta a)^m$, were 49.8 and 0.235 for DCB method, 53.175 and 0.221 for IFS method, where $K_R$ is the fracture resistance in $MPa\cdot m^{1/2}$ and $\Delta a$ is the crack extension length in meter. They proposed that the main toughening mechanisms should be the crack deflection and frictional pull-out of elongated β-grains. Pezzotti *et al.*[9] investigated monolithic $Si_3N_4$ sintered by HIP without sintering aids using IFS method. They observed no evidence of R-curve behavior. The slope of the straight line obtained by plotting log S (fracture strength) versus log P (indentation load) was almost-1/3, which suggested that the fracture resistance was almost independent of crack length. On the other hand, Ramachandran *et al.*[10] observed the R-curve behavior in a pressureless sintered $Si_3N_4$ by directly measuring the length of crack after Vickers indentation and IFS method. The slope of log S versus log P was-0.20. They proposed that the primary toughening mechanism was the formation of bridging ligaments by unbroken elongated β-$Si_3N_4$ grains right behind the advancing crack. Ritter *et al.*[11] observed $K_R$ in a pressureless sintered and annealed $Si_3N_4$ increased up to a crack size of ~1000 μm and proposed the crack bridging as a primary toughening mechanism. Very recently Choi *et al.*[12] also attributed the R-curve behavior to the bridging of the crack faces by the unbroken elongated β-grains.

In summary, controversy still remains as to what causes strong R-curve behavior in in-situ toughened $Si_3N_4$. In this study We obtained the complex microstructure consisted with large elongated β-grains dispersed in fine matrix grains by gas pressure sintering at 1950℃. Overall $K_R$ values increased drastically with strong R-curve characteristics. We found that crack bridging was primarily responsible for the R-curve behavior.

## 2. Experimental Procedure

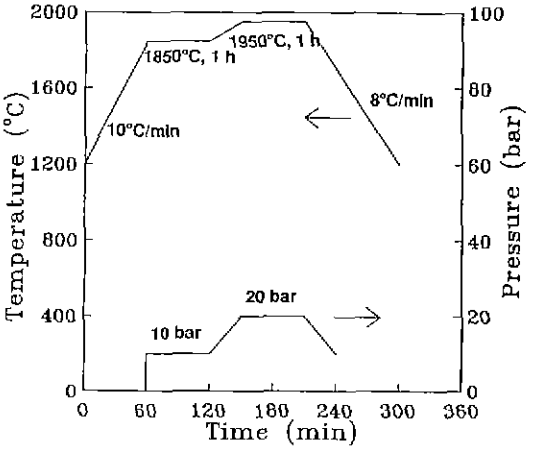


**Fig. 1.** Pressure and temperature schedule of gas-pressure sintering.

The $Si_3N_4$ powder* used in this experiment consisted of 98% of α phase with an average particle size of 0.35 μm and a specific surface area of 11 $m^2/g$. Amounts of additives were 3.9 wt% AlN and 6.4 wt% $Y_2O_3$. AlN and $Y_2O_3$ were added in the powder after making slurry with ethyl alcohol. The slurry was ball milled in a plastic container with $Si_3N_4$ balls, dried, and calcined at 650℃ for 5 h. Rectangular bars were prepared by pressing in a steel die and then isostatic pressing in a rubber bag under 250 MPa. The sintering was performed in a graphite furnace under pressurized nitrogen gas with the specimens placed in a BN-coated graphite crucible. Fig. 1 shows the pressure and temperature schedule used for sintering. The final density of the sintered specimens was measured by using the Archimedes' principle and showed theoretical density.

R-curves were determined by a controlled flaw/strength technique[13,14] using machined 3.0 mm×4.0 mm×40.0 mm bars. All specimen surfaces were polished with #1500 SiC emery paper, while the tensile surfaces were polished further with 0.25 μm diamond paste. The edges of the tensile surface were also beveled to remove edge cracks. Specimens were tested in a four-point bend fixture (inner span=20 mm and outer span=38 mm) on a mechanical testing machine at a crosshead speed of 0.5 mm/min. Prior to the testing, three Vickers indentations were placed on the tensile

*UBE SN-E-10, UBE Industries, Ltd., Tokyo, Japan.

surface of each bar in such a manner that the indentations were located between the inner loading points. The indentation loads varied from 19.6 to 294 N and loading time was 10 sec. Data was taken only for the specimens that fracture occurred from the indentation. Scanning electron microscope was used to examine the microstructure of the fractured surface. The crack lengths after indentation were measured by optical microscope. The half-length of the surface crack, $c_L$, was taken as the average of three indentation cracks.

### 3. R-Curve Analysis

R-curve analysis based on the controlled flaw/strength technique has been described by Cook *et al.*[13] and Krause[14]. In this analysis the fracture resistance, $K_R$, follows a power-law with the crack extension, $\Delta a$, such that

$$K_R = k(\Delta a)^m \tag{1}$$

where k and m are material constants. The exponent, m, is a measure of the susceptibility to R-curve behavior. It characterizes the rate at which $K_R$ increases with $\Delta a$. The coefficient k may be regarded as the intrinsic toughness of the material in the absence of any toughening mechanisms.

In order to determine k and m, we first measure the fracture strength (S) as a function of indentation load (P). Then we can determine $\alpha$ and $\beta$ using the following relationships.

$$S = \alpha P^{-\beta} \tag{2}$$

where the exponent $\beta$ is defined by

$$m = (1-3\beta)/(2+2\beta) \tag{3}$$

and the coefficient $\alpha$ is defined by

$$k = Y\alpha(\beta\gamma)^{-\beta}(1+\beta)^{(1+\beta)} \tag{4}$$

In Eq. (4), the constant Y is a dimensionless configuration coefficient that depends on specimen geometry and the constant $\gamma$ in Eq. (4) is defined by

$$\gamma = P/(a_i)^{2/(1-\beta)} \tag{5}$$

where $a_i$ is the initial crack depth due to indentation. The crack depth at the onset of instability, $a_f$, is given by

$$a_f = a_i[4/(1-2m)]^{2/(1+2m)} \tag{6}$$

For the case where $m=0$, $K_R$ is invariant with $\Delta a$, and $\beta = 1/3$. These special conditions represent flat R-curve behavior.

A R-curve is generated by firstly taking the logarithm of Eq. (2) and plotting log (S) versus log (P). From this plot, the constants $\alpha$ and $\beta$ can be determined from the intercept and slope, repectively. The constants m and k can then be calculated utilizing Eq. (3) and (4), respectively. In calculating constant k, it is necessary to determine the constant $\gamma$. For this calcu-

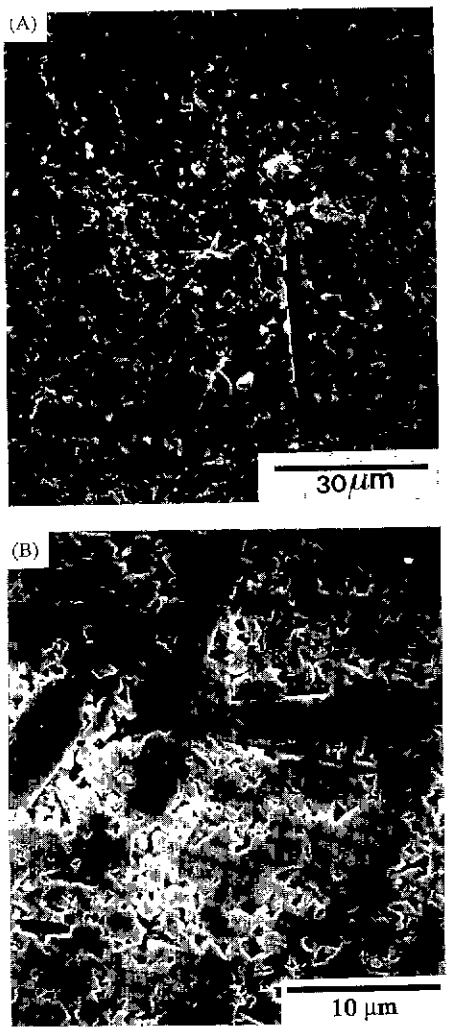


**Fig. 2.** Scanning electron micrographs of (A) a fractured and (B) a polished surface of the gas-pressure sintered $Si_3N_4$.

**Table 1.** Summary of Data From the Controlled Flaw/Strength Measurement.

| P# (N) | C* (μm) | S+ (MPa) |
|---|---|---|
| 19.6 | 31 | 741 |
| 49 | 58 | 596 |
| 98 | 87 | 531 |
| 196 | 148 | 432 |
| 294 | 189 | 385 |

#indentation load, *crack length, +fracture strength

lation, Eq. (5) is utilized with the assumption that $a_1$ is identical with $c_i$, which is the initial crack length measured from the specimen surface after indentation. With the use of Eq. (1), a plot of $K_R$ versus $\Delta a$ can be made, where $\Delta a = a_T$, as given by Eq. (6).

## 4. Results

The microstructures of a gas-pressure sintered $Si_3N_4$ are shown in Fig. 2. They revealed the bimodal structure with large elongated β-grains dispersed in equiaxed matrix grains. The average aspect ratio of large β-grains was approximately 8 with the average length ~20 μm and the average diameter ~2.5 μm.

The results of indentation and four-point-bending tests are presented in Table 1, and plotted in Fig. 3. A linear least-squares fit of the data shown in Fig. 3 gave $\alpha = 1524.05$ and $\beta = 0.239$. Since the value of $\beta$ is approximately 30% less than the 1/3, a rising R-curve is evident. Assuming $a_1 = c_i$, the constant $\gamma$ was determined as $\gamma = 3.332 \times 10^8$, which gives $m = 0.115$ and $k = 30.301$, assuming $Y = 1.174$[13].

Cook *et al.*[15] have in fact demonstrated that many brittle materials exhibit a distinct cruvature in the fracture strength-indentation load response. However, over the range of indentation loads utilized in this investigation, there appreared to be a linear relationship between log S and log P as shown in Fig. 3.

Fig. 4 shows R-curves determined in this study. The results reported in the literature are also included in the figure. The $K_R$ measured in this work are higher than others reported. Our value of $K_R$ rises steeply up to ~300 μm of crack length and increases almost linearly afterward.

## 5. Discussion

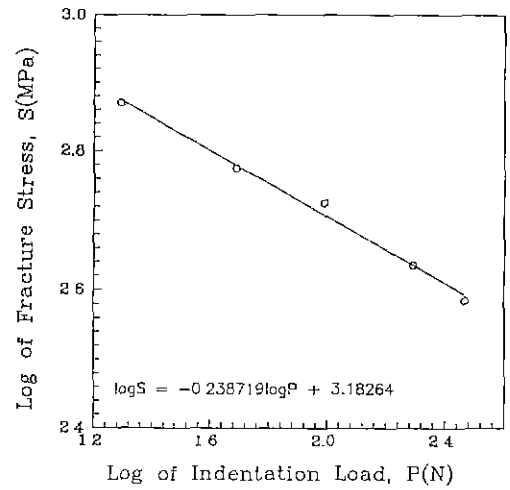


**Fig. 3.** Logarithm of fracture strength (S) versus logarithm of indentation load (P). A linear least-squares fit of Eq. (2) is shown and its slope is −0.238719.

As discussed in the introduction, various mechanisms have been proposed to be contributing the R-curve characteristics in monolithic silicon nitride. They are crack deflection[6-8], frictional pull-out of β-grains[8,16], and the bridging by unbroken β-grains in the crack wake[10-12]. Attempts were made to identify the dominant mode of microstructural processing that might contribute significantly to the R-curve characteristics shown in Fig. 4.

First of all, the contribution of frictional pull-out seems to be negligible in our $Si_3N_4$ ceramics. In order to have a frictional pull-out of β-grains operational, frictional interfaces between β-grains and matrix grains have to be developed presumably as a result of the situation illustrated in Fig. 5(A). Exhaustive search for such cases failed to identify any evidence of the situation in Fig. 5(A). Whereas, the situation illustrated in Fig. 5(B) has been frequently observed as presented in the microstructure shown in Fig 5(C). Attempts to find the situation shown in Fig. 5(A) using the fracture surface also failed to identify the pull-out mechanism. The toughening due to the frictional pull-out of broken whisker has been identified convincingly in $Al_2O_3$-SiC whisker composite[3]. The increase in toughness due to the frictional pull-out of whiskers depends not only on the size and spacing of whiskers but more importa-

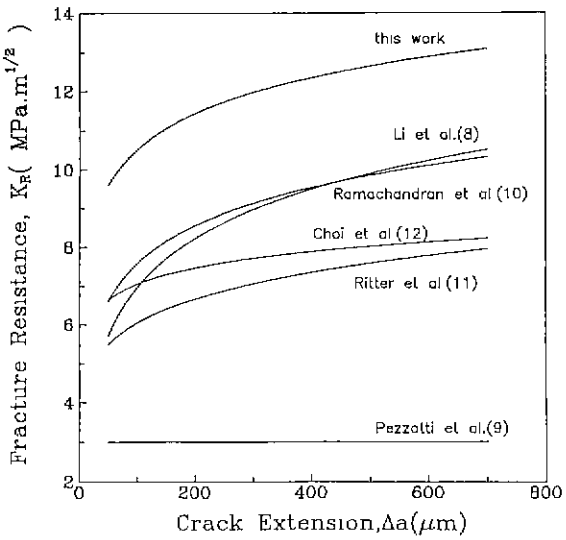


**Fig. 4.** Fracture resistance ($K_R$) versus crack extension (Δa) illustrating rising R-curve behavior in the gas-pressure sintered $Si_3N_4$. Other data are included for the comparison.

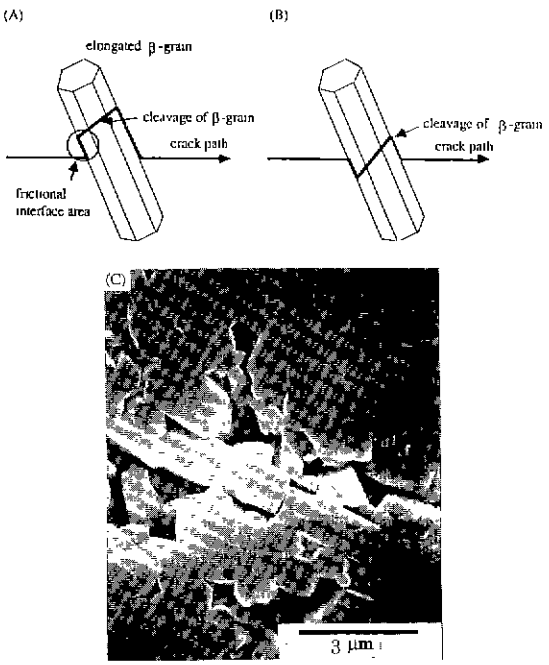


**Fig. 5.** (A) Schematic illustration of the crack path which induces frictional pull-out of broken β-grains, (B) such crack path would not develop the pull-out process, (C) the microstructural evidence which support the case in (B).

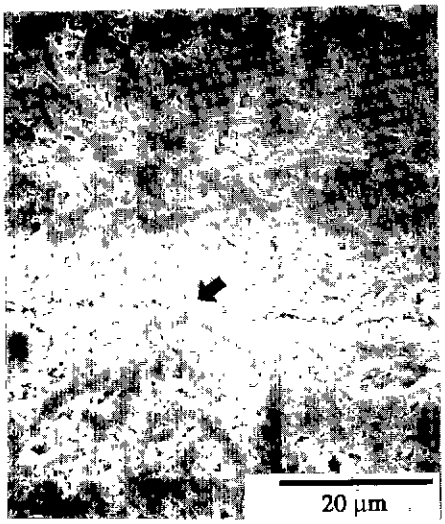


**Fig. 6.** Scanning electron micrograph of the crack path which shows the evidence of bridging β-grains.

ntly also on the thermal expansion coefficient mismatch and the interfacial characteristics between the matrix and whisker[16]. In-situ grown β-grains in $Si_3N_4$ are tightly inter-locked with matrix grains in the course of α-β phase transformation and β-grain growth. Hence, it is unlikely that the microstructural conditions illustrated in Fig. 5(A) could be developed in $Si_3N_4$.

The toughness increase due to crack deflection[6-8] have been discussed as an alternative microstructural process in front of crack tip region. It is a viable mechanism. However, suppose the large elongated β-grains play dominant role of deflecting the crack growth path as illustrated in Fig. 5(B), then the critical crack length (Δa) below which R-curves rise steeply would be in the order of the spacing between β-grains. The microstructures shown in Fig. 2 revealed that the average spacing between β-grains that could be experienced by the running crack should not be larger than 20~30 μm. However, the critical crack length estimated from the R-curves measured is in the order of 300 μm. Therefore, we can exclude the crack deflection from the dominant microstructural processes which brings forth the R-curve characteristic measured in our $Si_3N_4$. However, we cannot rule out the possibility of contribution of crack deflection on R-curve particularly near the crack tip region. R-curve in the range $\Delta a <$ 20~30 μm has to be measured in order to confirm

**Table 2.** Summary of the Microstructural Parameters of the Monolithic $SI_3N_4$ Used for Measruing R-curves.

| | average aspect ratio | β-grain length (μm) | β-grain diameter (μm) | morphology | process |
|---|---|---|---|---|---|
| Li *et al.*[8] | ~8 | ~40 | ~5 | highly bimodal | GPS* |
| Pezzotti *et al.*[9] | | unknown | | homogeneous | HIP# |
| Ramachandran *et al.*[10] | ~5 | ~5 | ~1 | bimodal | Pressureless sintering |
| Ritter *et al.*[11] | ~8 | ~40 | ~5 | highly bimodal | Pressureless sintering and annealing |
| Choi *et al.*[12] | ~5 | ~10 | ~2 | bimodal | GPS |
| This work | 8~10 | 20~25 | 2~3 | highly bimodal | GPS |

*GPS: gas pressure sintering, #HIP: hot isostatic pressing

it.

On the other hand, bridging by unbroken β-grains in the crack wake seems to be actively operating according to the microstructural observation around the crack tip region. Fig. 6 shows a typical example of bridging grains. The bridging mechanism has been identified firstly by Swanson *et al.*[17] in coarsed-grain alumina. Lately, Lawn *et al.*[18] analyzed the R-curve characteristics of R-curve in terms of bridging mechanism and explained the continuously rising R-curve even up to a few mm of crack length in polycrystalline alumina. It is difficult to apply the analysis by Lawn *et al.* to $Si_3N_4$ without knowing the various microstructural parameters such as the number density of active bridging grains. However, the fact that R-curve observed in this study rises fast up to about 300 μm and continuously increases up to about 1 mm of crack length is consistent with the experimental observation on R-curve behaviors of alumina and with the analysis based on the bridging mecharism.

Now the remaining question is what is the optimal microstructure to enhance toughening in monolithic $Si_3N_4$. The results of Tajima *et al.*[19] show that the toughening contribution by crack bridging increases with increase in volume content of the elongated grains. More recent observations[16] also reveal that the bridging contribution increases with increase in the cross-sectional dimension of the elongated grains—fracture toughness proportional to the square root of grain diameter. Briefly speaking, the larger the diameter and the volume fraction of the elongated β-grains are, the better the toughness improvement will be.

However, the key to the in $K_R$ is how effectively β-grains become active as bridging ligaments during crack growth. It depends largely on the interfacial characteristics between β-grains and the matrix. The reason is not clear why our R-curves is significantly higher than others with similar microstructural conditions. Table 2 compares several microstructural parameters related to the R-curves shown in Fig. 4. Any significant correlations could not be established. It seems that interfacial chemistry plays an important role for the development of bridging ligament in $Si_3N_4$ which shows the duplex microstructure of large β-grains in small matrix grains. GPS (gas pressure sintering) seems to be effective in obtaining such microstructure. hence, it is suggested to study the effect of additives on R-curve characteristic using GPS technique.

## 6. Summary

The gas pressure sintering was efficient in obtaining the in-situ toughened $Si_3N_4$ which is chracterized by large elongated β-grains dispersed in fine matrix grains. The R-curve measured by controlled flaw/strength technique was similar to others reported previously, but interestingly the fracture resistance ($K_R$) was significantly higher than any values reported. Analysis of R-curves and microstructure around the crack tip region suggested that the bridging mechanism by unbroken β-grain ligament in the crack wake was the prime toughening process that gave rise to the R-curve determined up to about 1 mm of crack advance. Whe-

reas, the contribution by crack deflection by β-grains should be limited only near crack tip region up to 20~30 μm of crack length.

## REFERENCES


1. M.V. Swain and R.H.J. Hannik, "R-Curve Behavior of Zirconia Ceramics," pp. 225-239 in Advances in Ceramics, Vol. 12, Science and Technology of Zirconia II, Edited by N. Claussen, M. Ruhle, and A.H. Heuer, Am. Ceram. Soc. Columbus, OH, 1984.
2. D.B. Marshall, "Strength Characteristics of Transformation-Toughened Zirconia," *J. Am. Ceram. Soc.*, **69**(3), 173-180 (1986).
3. R.F. Krause, E.R. Fuller, and J.F. Rhodes, "Fracture Resistance Behavior of Silicon Carbide Whisker-Reinforced Alumina Composites with Different Porosities," *J. Am. Ceram. Soc.*, **73**(3), 559-566 (1990).
4. A. Reichl and R.W. Steinbrech, "Determination of Crack-Bridging Forces in Alumina," *J. Am. Ceram. Soc.*, **71**(6), C-299-C-301 (1988).
5. G. Himsolt, H. Knoch, H. Huebner, and F.W. Kleinlein, "Mechanical Properties of Hot-Pressed Silicon Nitride with Different Grain Structures," *J. Am. Ceram. Soc.*, **62**(1-2), 29-32 (1979).
6. F.F. Lange, "Relation Between Strength, Fracture Energy, and Microstructure of Hot-Pressed $Si_3N_4$," *J. Am. Ceram. Soc.*, **56**(10), 518-522 (1973).
7. E. Tani, S. Umebayashi, K. Kishi, K. Kobayashi, and M. Nishijima, "Gas-Pressure Sintering of $Si_3N_4$ with Concurrent Addition of $Al_2O_3$ and 5 wt% Rare Earth Oxides: High Fracture Toughness $Si_3N_4$ with Fiber-Like Structure," *Am. Ceram Soc. Bull.*, **65**(9), 1311-1315 (1986).
8. C.W. Li and J. Yamanis, "Super-Tough Silicon Nitride with R-Curve Behavior." *Ceram. Eng Sci. Proc*, **10**(7-8), 632-645 (1989).
9. G. Pezzotti, I. Tanaka, and T. Okamoto. "$Si_3N_4$/SiC-Whisker Composites Without Sintering Aids: II, Fracture Behavior," *J. Am. Ceram. Soc.*, **73**(10), 3039-3045 (1990).
10. N. Ramachandran and D.K. Shetty, "Rising Crack-Growth-Resistance (R-Curve) Behavior of Toughened Alumina and Silicon Nitride," *J. Am. Ceram. Soc.*, **74** (10), 2634-2641 (1991).
11. J.E. Ritter, S.R. Choi, K. Jakus, P.J. Whalen, and R.G. Rateick, "Effect of Microstructure on the Erosion and Impact Damage of Sintered Silicon Nitride," *J. Mater. Sci*, **26**, 5543-5546 (1991).
12. S.R. Choi, J.A. Salem, and W.A. Sanders, "Estimation of Crack Closure Stresses for In Situ Toughened Silicon Nitride with 8 wt% Scandia," *J. Am. Ceram. Soc.*, **75**(6), 1508-1511 (1992).
13. R.F. Cook and D.R. Clark, "Fracture Stability, R-Curves and Strength Variability," *Acta Metall.*, **36**(3), 555-562 (1988).
14. R.F. Krause, "Rising Fracture Toughness from the Bending Strength of Indented Alumina Beams," *J. Am. Ceram. Soc*, **71**(5), 338-343 (1988).
15. R.F. Cook, B.R. Lawn, and C.J. Fairbanks, "Microstructure-Strength Properties in Ceramics: I, Effect of Crack Size on Toughness," *J. Am. Ceram. Soc.*, **68**(11), 604-615 (1985).
16. P.F. Becher, "Microstructural Design of Toughened Ceramics," *J. Am. Ceram. Soc.*, **74**(2), 255-269 (1991).
17. P.L. Swanson, C.J. Fairbanks, B.R. Lawn, Y. Mai, and B.J. Hockey, "Crack-Interface Grain Bridging as a Fracture Resistance Mechanism in Ceramics: I, Experimental Study on Alumina," *J. Am Ceram. Soc.*, **70**(4), 279-289 (1987).
18. P. Chantikul, S.J. Bennison, and B.R. Lawn, "Role of Grain Size in the Strength and R-Curve Properties of Alumina," *J Am. Ceram. Soc.*, **73**(8), 2419-2427 (1990).
19. Y. Tajima, K Urashima, M. Watanabe, and Y. Matsuo, "Fracture Toughness and Microstructure Evaluation of Silicon Nitride Ceramics"; pp. 1034-1041 in Ceramic Transactions, Vol. 1, Ceramic Powder Science-IIB. Edited by G.L. Messing, E.R. Fuller, Jr., and H. Hansner, American Ceramic Society, Westerville, OH, 1988.